Concurrent Application of Energy-Based Modeling Methodologies to Dynamics Analysis and Control: The Case of a Robotic Omnidirectional Base

Martín Crespo
LAC - FCEIA
Universidad Nacional de Rosario
Rosario, Argentina
crespom@fceia.unr.edu.ar

Sergio Junco
LAC - FCEIA
Universidad Nacional de Rosario
Rosario, Argentina
sjunco@fceia.unr.edu.ar

Matías Nacusse
LAC - FCEIA
Universidad Nacional de Rosario
Rosario, Argentina
nacusse@fceia.unr.edu.ar

***Abstract*—The purpose of this paper is to show the benefits of approaching the tasks of analysis, simulation and control system design through the consideration of system properties via the concurrent approach of different modeling methodologies. The particular case of an omnidirectional robotic base is chosen to present the approach in an illustrative way. The presentation of its differential kinematics is followed by the derivation of the dynamic models under different modeling approaches: the Bond Graphs, Euler-Lagrange, Newtonian and port-Hamiltonian paradigms. Using the Bond Graphs as a guiding thread, equivalences among the models are obtained which are further used to reinterpret system properties when considering them from the point of view of different formalisms, and also to bring to light some properties that may be hidden in some cases. The paper concludes by designing a velocity controller for the mobile platform starting with a physically heuristic approach on its Bond Graph model and, subsequently, demonstrating its stability in the port-Hamiltonian domain using the correspondences previously established concerning passivity under feedback interconnection.**

***Index Terms*—Dynamic Models, Mobile Robots, Bond Graphs, Euler Lagrange, port-Hamiltonians, Omni Wheels.**

I. Introduction

Mathematical Modeling plays an ever increasing role in Engineering, where the use of physical, behavioral and logical models in conjunction with software tools and methodologies brought-in approaches like Model-Based Systems Engineering (MBSE), the formalized application of modeling to support system requirements, design, analysis, verification and validation activities beginning in the conceptual design phase and continuing throughout development and later life cycle phases [1].

Model-Based Design (MBD), a component of MBSE, is a key methodology in Mechatronics, where a plethora of model types and techniques are mandatory due to the profusion of physical domains, engineering disciplines and technologies involved [2]. Among this multitude of types of models conspicuous in Mechatronics, for each specific task mostly just a single type of model is used, even if more than one are available. Particularly in the domain of control and automation, where dynamic physical models are of uppermost importance, some modeling methodologies are preferred, according to well-established practices (and/or to the taste of the developers). For instance, the Euler-Lagrange (EL) formalism is the main technique recurred to in Robotics, despite the existence of the also well-established Newton-Euler formulation, or the more recently irrupted alternative techniques as, for instance, the port-Hamiltonian System (pHS) approach.

The EL and pHS models are natural candidates for describing numerous physical systems, as they capture the energy phenomena associated with the physical-based laws, such as (i) storage, (ii) flow, and (iii) dissipation. [3] [4]. We also consider the Bond Graphs (BG), a graphical representation that allows capturing energy phenomena as well as causal relationships between system variables, and is a highly suitable tool primarily conceived for modeling and simulation [5] and later also exploited for controller design [6] [7].

The purpose of this paper is to show that the benefits of a single-modeling approach to the tasks of analysis, simulation and control system design can be advantageously extended and deepened through the consideration of system properties via the concurrent approach of different methodologies. To this aim, the EL, Newton, pHS and BG modeling paradigms will be considered, as applied to the particular case of a mobile omnidirectional robotic platform. Such robots are called omnidirectional because they possess full mobility in the plane which means that they can move at each time instant in any direction without any reorientation [8].

In [9] the BG methodology was used for the development of the dynamic model and control for a mobile manipulator. In [10] a 3D dynamic model of a quadruped robot has been developed using the BG technique. In [11] a BG model of a planar mobile manipulator is presented in correspondence with its EL, BG with storage fields, and pHS models for analysis simulation and control. In [12] and [13] a systematic methodology to convert BG models to EL and pHS is presented respectively. The work [14] achieves a correspondence between port-based modeling of multi-domain physical systems using BG with the framework of geometric dynamical systems and control theory using pHS.

The remainder of this paper is organized as follows. In Section II the kinematics and dynamics of the omnidirectional mobile base is presented. Section III, Equivalences and Synergies, discusses correspondences among these models and exploits them in order to gain insight into system properties and to inspire and facilitate controller design. Section IV presents an application of the previous ideas via the development of a velocity controller for the mobile platform. Finally, the conclusions are discussed in Section V.

II. Modeling the Mobile Base

A. Differential Kinematics

In Fig. 1a, the idealized physical system of an omnidirectional mobile base is depicted. It is composed of a main rigid body, henceforth referred to as the chassis, and three wheels (each of them, in turn, a rigid body), located 120 degrees apart from each other. The variables describing the motion of the center of mass (CM) of the base are the generalized independent coordinates (posture) $q = [x,\, y,\, \varphi]^T$ with respect to the fixed global system $O - X_F Y_F Z_F$ and the vector $\eta = [\dot{X}_G,\, \dot{Y}_G,\, \dot{\varphi}]^T$ that represents the non-inertial velocities of the CM of the chassis defined with respect to the non-inertial frame $O_G - X_G Y_G Z_G$. The vector of efforts $h_e = [F_{ex},\, F_{ey},\, \tau_e]^T$ represents the external forces exterted at the CM of the chassis.

From the idealized scheme of omni wheel i, with $i = 1, 2, 3$, shown in Fig. 1b, the non-inertial rotational velocities $\Omega_r = [\Omega_{r1},\, \Omega_{r2},\, \Omega_{r3}]^T$ and translational velocities $V_r = [V_{r1},\, V_{r2},\, V_{r3}]^T$ are identified, both defined with respect to the moving frame $O_{ri} - X_{ri} Y_{ri} Z_{ri}$, and the external torques (coming from motors) $\tau = [\tau_{r1},\, \tau_{r2},\, \tau_{r3}]^T$.

As the movement of the base depends on the wheels, the velocities $\dot{q}$ and V_r are not independent of each other, but rather are related to η through the relationships

$$\begin{cases} \dot{q} = R(q)^T \eta \\ V_r = rE\eta \end{cases} \quad \Rightarrow \quad V_r = rER(q)\dot{q} \tag{1}$$

where r is the radius of the wheels, L is the distance from the CM of the chassis to the wheel axis, and the matrices[1]

$$R(q) = \begin{bmatrix} c_\varphi & s_\varphi & 0 \\ -s_\varphi & c_\varphi & 0 \\ 0 & 0 & 1 \end{bmatrix} \quad E = \begin{bmatrix} 1/2r & \sqrt{3}/2r & L/r \\ -1/r & 0 & L/r \\ 1/2r & -\sqrt{3}/2r & L/r \end{bmatrix}$$

taking into account that $R(q)R(q)^T = \boldsymbol{I}_3$.

If we consider that the motion of the wheel occurs under conditions of perfect rolling and without slipping around the vertical axis passing through the contact point, the velocity vector V_r can be expressed as

$$V_r = r\Omega_r \tag{2}$$

[1]The notations c_φ and s_φ are the abbreviations for $\cos\varphi$ and $\sin\varphi$, respectively.

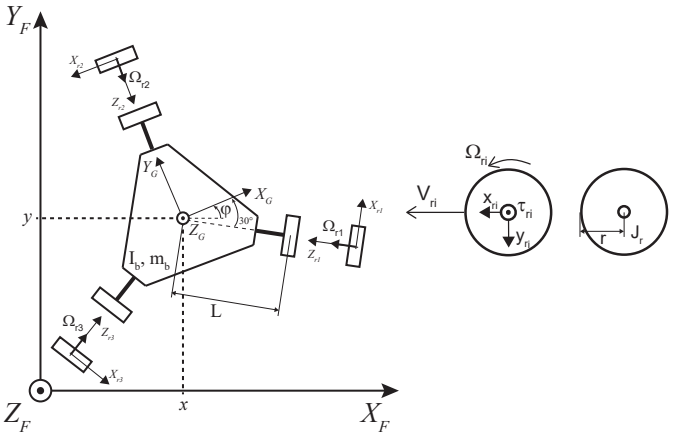

(a) Idealized physical model.

(b) Velocities and parameters of wheel i.

Fig. 1: Omnidirectional mobile base.

Thus, by substituting into (1), we obtain the kinematic relationship between the frame $O - X_F Y_F Z_F$ and the frames $O_{ri} - X_{ri} Y_{ri} Z_{ri}$

$$\Omega_r = G(q)^T \dot{q} \tag{3}$$

where the matrix $G(q)$ has been defined as $G(q) := R(q)^T E^T$.

B. Dynamics

In this section, we develop the dynamic model of the mobile base through four different methodologies: BG, force balance or Newtonian method, EL equations, and pHS.

1) Bond Graph: The velocity relationship of equation (3) is represented in the BG domain by interconnecting the **1**-junctions associated with these velocities through the modulated transformer **MTF**. Effort sources **Se** are used to represent external forces and torques.

The causalized BG model is presented in Fig. 2, where the convention of positive power flow is taken from the wheels to the chassis. The three parts of the model are clearly distinguished: the omni wheels, the relationship between the inertial velocities, and the chassis. The **I** elements represent the rotational inertia of the wheels J_r, and the mass and inertia of the base, m_b and I_b respectively.

The vectors $F = [F_x,\, F_y,\, \tau_1]^T$ and $F_r = [F_{r1},\, F_{r2},\, F_{r3}]^T$ represent internal efforts and traction forces on the wheels, respectively, related in a power-conserving transformation such that

$$\begin{cases} \Omega_r = G(q)^T \dot{q} \\ F = G(q) r F_r \end{cases} \tag{4}$$

Remark 1. The order of the BG scheme is $n_{BG} = 6$, as it possesses three energy storage elements in integral causality (IC) and an integrator in a three dimensional vector. The state variables of the system are the momentum quantities associated with the energy storage elements in IC and the generalized independent posture coordinates q.

2) Force Balance: The differential equations describing the dynamics of the mobile base in the fixed global framework, and the rotational dynamics of the wheel-motor assembly in their respective local frames, can be obtained through Newton's second law by examining the force balance.

$$\begin{cases} M_b\ddot{q} = F + h_e \\ I_r\dot{\Omega}_r = \tau - rF_r \end{cases} \tag{5}$$

where $M_b = \text{diag}\{[m_b,\ m_b,\ I_b]\}$ and $I_r = \text{diag}\{[J_r,\ J_r,\ J_r]\}$. On the other hand, by taking the derivative of (3) with respect to time, we obtain

$$\dot{\Omega}_r = G(q)^T\ddot{q} + \dot{G}(q)^T\dot{q} \tag{6}$$

Thus, solving rF_r from (5) and substituting it into the second line of (4) yields

$$F = G(q)\left(\tau - I_r\dot{\Omega}_r\right)$$

Then, substituting $\dot{\Omega}_r$ with (6), F in the first line of (5), and rearranging we obtain the dynamical model

$$M(q)\ddot{q} + C(q,\dot{q})\dot{q} = G(q)\tau + h_e \tag{7}$$

where $M(q) = M_b + G(q)I_rG(q)^T$ is the inertia matrix, symmetric and positive definite, and $C(q,\dot{q})\dot{q} = G(q)I_r\dot{G}(q)^T$ is a term encompassing centrifugal and Coriolis torques/forces. The expressions for the matrices are:

$$M(q) = \begin{bmatrix} \frac{3J_r}{2r^2} + m_b & 0 & 0 \\ 0 & \frac{3J_r}{2r^2} + m_b & 0 \\ 0 & 0 & \frac{3J_rL^2}{2r^2} + I_b \end{bmatrix} \tag{8}$$

$$C(q,\dot{q}) = \begin{bmatrix} 0 & \frac{3J_r}{2r^2}\dot{\varphi}_0 & 0 \\ -\frac{3J_r}{2r^2}\dot{\varphi}_0 & 0 & 0 \\ 0 & 0 & 0 \end{bmatrix}$$

Remark 2. Since the product $G(q)I_rG(q)^T$ is constant, from now on, the dependence of the inertia matrix on the vector q will be omitted.

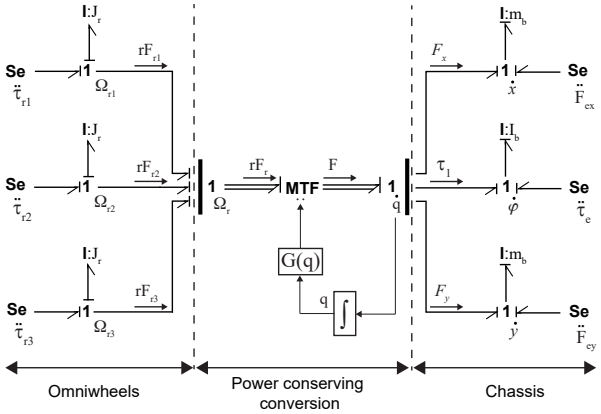

Fig. 2: Causalized BG model of the omnidirectional mobile base.

3) Euler Lagrange: The Lagrangian $\mathcal{L}$ of the mobile base is

$$\begin{aligned} \mathcal{L}(\psi,\dot{\psi}) &= \frac{1}{2}\dot{q}^TM_b\dot{q} + \frac{1}{2}\Omega_r^TI_r\Omega_r \\ &= \frac{1}{2}\dot{\psi}^TB\dot{\psi} \end{aligned} \tag{9}$$

where $B = \text{diag}\{[M_b,\ I_r]\}$ is the augmented inertia matrix (also symmetric and positive definite), and $\dot{\psi} = \left[\dot{q}^T,\ \Omega_r^T\right]^T$, being ψ the configuration coordinates.

Remark 3. From expression (9), it can be seen that the configuration coordinates ψ are cyclic (or ignorable) since they do not appear in the Lagrangian expression.

With the EL formulation, the equations of motion can be generated systematically, regardless of the adopted frame of reference. Then, the general formulation of the EL equations for a system that possesses kinematic constraints is [15]

$$\frac{d}{dt}\left(\frac{\partial\mathcal{L}}{\partial\dot{\psi}}\right) - \frac{\partial\mathcal{L}}{\partial\psi} = S(\psi)u + A(\psi)\lambda, \quad u\in\mathbb{R}^6,\ \lambda\in\mathbb{R}^3 \tag{10}$$

where λ is the vector of Lagrange multipliers (also called the vector of restrictive forces [16]) and

$$S(\psi) = \begin{bmatrix} \boldsymbol{I}_3 & \boldsymbol{0}_3 \\ \boldsymbol{0}_3 & \boldsymbol{I}_3 \end{bmatrix} \quad u = \begin{bmatrix} h_e \\ \tau \end{bmatrix} \quad A(\psi) = \begin{bmatrix} G(q) \\ -\boldsymbol{I}_3 \end{bmatrix} \tag{11}$$

Using (9) and (10), the dynamic model of the constrained mechanical system is obtained as

$$\begin{aligned} B\ddot{\psi} &= S(\psi)u + A(\psi)\lambda \\ A(\psi)^T\dot{\psi} &= \boldsymbol{0}_{3\times1} \end{aligned} \tag{12}$$

Let's consider the matrix $J(\psi) = [\boldsymbol{I}_3,\ G(q)]^T$ whose columns form the basis of the null space of $A(\psi)^T$, i.e., $A(\psi)^TJ(\psi) = 0$. Thus, replacing the constraints in (12) with

$$\dot{\psi} = J(\psi)\dot{q} \tag{13}$$

and by pre-multiplying both sides of equation (12) by $J(\psi)^T$, we arrive at the reduced dynamic model

$$J(\psi)^TB\ddot{\psi} = J(\psi)^Tu \tag{14}$$

Then, differentiating (13) with respect to time and substituting the expression for $\ddot{\psi}$ in the reduced dynamic model (14), we obtain the same model as equation (7), where it is satisfied that

$$M = J(\psi)^TBJ(\psi) \quad C(q,\dot{q}) = J(\psi)^TB\dot{J}(\psi) \tag{15}$$

4) Hamiltonian System: The Hamiltonian equations are derived from the EL equations starting from the definition of the generalized momentum

$$p := \frac{\partial\mathcal{L}}{\partial\dot{\psi}}$$

and from the Hamiltonian, representing the total energy, through the Legendre transformation of the Lagrangian

$$\mathcal{H}(\psi,p) := p^T\dot{\psi} - \mathcal{L}(\psi,\dot{\psi})$$

Thus, the Hamiltonian equations of a general system with constraints are

$$\begin{aligned}\dot{\psi} =&\frac{\partial H}{\partial p}(\psi,p)\\ \dot{p} =&-\frac{\partial H}{\partial \psi}(\psi,p)+S(\psi)u+A(\psi)\lambda\\ y =&S(\psi)^T\frac{\partial H}{\partial p}(\psi,p)\\ \mathbf{0}_{3\times 1} =&A(\psi)^T\frac{\partial H}{\partial p}(\psi,p)\end{aligned} \tag{16}$$

where y is the *co-llocated output* (i.e., it has relative degree 1 with respect to the control input u). In this particular case, the momentum and the Hamiltonian are:

$$p = B\dot{\psi} \quad H(\psi,p)=\frac{1}{2}p^TB^{-1}p \tag{17}$$

and the values of the matrices $S(\psi)$ and $A(\psi)$ are as expressed in (11). Taking into account that the Lagrange multipliers can be eliminated by multiplying both sides of the second line of (16) by $J(\psi)^T$, we obtain

$$J(\psi)^T\dot{p} = -J(\psi)^T\frac{\partial H}{\partial \psi}(\psi,p)+J(\psi)^TS(\psi)u \tag{18}$$

Let's now define $\tilde{p}\in\mathbb{R}^3$ through the following change of coordinates (see [4])

$$\tilde{p} :=J(\psi)^Tp$$

where considering both, the equation (15) and that the momentum can be rewritten as $p = BJ(\psi)\dot{q}$, the Hamiltonian (17) can be expressed in terms of the new coordinates $\tilde{p}$ as

$$\tilde{H}(\psi,\tilde{p})=\frac{1}{2}\tilde{p}^TM^{-1}\tilde{p} \tag{19}$$

Then, differentiating $\tilde{p}$ with respect to time, the equation (18) can be rewritten as

$$\dot{\tilde{p}} = -J(\psi)^T\frac{\partial H}{\partial \psi}(\psi,p)+\dot{J}(\psi)^Tp+J(\psi)^TS(\psi)u$$

As it holds that

$$\frac{\partial H}{\partial p}=\frac{\partial \tilde{H}}{\partial \tilde{p}}=\dot{q} \qquad \frac{\partial H}{\partial \psi}=\frac{\partial \tilde{H}}{\partial \psi}=\mathbf{0}_{6\times 1} \tag{20}$$

the constrained system (16) takes the form

$$\begin{bmatrix}\dot{\psi}\\ \dot{\tilde{p}}\end{bmatrix}=\left[\begin{array}{c|c}\mathbf{0}_6 & J(\psi)\\ \hline -J(\psi)^T & \dot{J}(\psi)^TBJ(\psi)\end{array}\right]\begin{bmatrix}\frac{\partial \tilde{H}}{\partial \psi}\\ \frac{\partial \tilde{H}}{\partial \tilde{p}}\end{bmatrix}+\begin{bmatrix}\mathbf{0}_6\\ J(\psi)^T\end{bmatrix}u$$

$$y=\begin{bmatrix}\mathbf{0}_6 & J(\psi)\end{bmatrix}\begin{bmatrix}\frac{\partial \tilde{H}}{\partial \psi}\\ \frac{\partial \tilde{H}}{\partial \tilde{p}}\end{bmatrix}$$

where in this case, the output are the velocities $y=\dot{\psi}$.

Now, since the Hamiltonian $\tilde{H}$ depends on the inertia matrix M which, in the general case, depends on the vector of posture coordinates q, it is possible to express the Hamiltonian $\tilde{H}$ in terms of q and $\tilde{p}$. Thus, considering the equivalences of (20) and defining the state vector as $\mathbf{x} := \begin{bmatrix}q^T,\ \tilde{p}^T\end{bmatrix}^T$, the simplified dynamic system is[2]:

$$\begin{aligned}\begin{bmatrix}\dot{q}\\ \dot{\tilde{p}}\end{bmatrix}=&\underbrace{\left[\begin{array}{c|c}\mathbf{0}_3 & \boldsymbol{I}_3\\ \hline -\boldsymbol{I}_3 & -C(q,\dot{q})\end{array}\right]}_{\mathrm{J}(\boldsymbol{x})}\begin{bmatrix}\frac{\partial \tilde{H}}{\partial q}\\ \frac{\partial \tilde{H}}{\partial \tilde{p}}\end{bmatrix}+\underbrace{\begin{bmatrix}\mathbf{0}_3 & \mathbf{0}_3\\ \boldsymbol{I}_3 & G(q)\end{bmatrix}}_{\mathrm{g}(\boldsymbol{x})}u\\ y=&\begin{bmatrix}\mathbf{0}_3 & \boldsymbol{I}_3\\ \mathbf{0}_3 & G(q)^T\end{bmatrix}\begin{bmatrix}\frac{\partial \tilde{H}}{\partial q}\\ \frac{\partial \tilde{H}}{\partial \tilde{p}}\end{bmatrix}\end{aligned} \tag{21}$$

where the second equality of equation (15) together with the antisymmetry property $C(q,\dot{q})^T=-C(q,\dot{q})$ have been used. The skew-symmetric matrix $J(\mathbf{x})=-J(\mathbf{x})^T$, of dimension (6×6) reveals the power conservation of the interconnection structure. Finally, the compact pHS model of the mobile base is:

$$\begin{aligned}\dot{\boldsymbol{x}} &= J(\boldsymbol{x})\nabla\tilde{H}(\boldsymbol{x})+g(\boldsymbol{x})u\\ y &= g(\boldsymbol{x})^T\nabla\tilde{H}(\boldsymbol{x})\end{aligned}$$

III. Model Analysis

In this section, we will use modeling in the BG domain as a basis to establish connections and interpretations between the different developed models.

Recurring to the assignment of computational causality, BGs are mainly used for computational purposes, both numerical, i.e., digital simulation, and analytical, i.e., differential equations derivation, mainly state equations [5] but also EL [12] and pHS [13]. The formal procedures to do this start from either BGs in full IC and without algebraic loops, or from BGs including derivative causality (DC), like the one in Fig. 2, and algebraic loops.

In both latter cases differential-algebraic equations (DAE-systems) are implied with index equal or greater than one [17]. To avoid dealing with them, different approaches are available. When possible, the conversion of the DAE-system to a pure ODE (an index zero system) through formal manipulation is preferred. When not, the addition to the BG of parasitic dynamic components or residual sinks [18] are other options on hand allowing to break the causal couplings producing the DAE-system.

In the sequel some of these techniques are applied to the BG of Fig. 2 and some implications related to the models in the different formalisms are discussed.

A. DAE to ODE conversion and BG-EL-Force-balance correspondences

Eliminating the presence of energy storage elements in DC in a BG via regrouping the interdependent storage elements is equivalent to converting a DAE-system to a index zero system.

[2]Notice that $\dot{q}$ can be expressed in terms of $\tilde{p}$, so the interconnection matrix depends on the state $\mathbf{x}$.

In the case of the BG shown in Fig. 2, this regrouping involves moving the rotational inertias of the wheels that are in DC to the right side, so that all energy storage elements are in IC, as shown in the BG schematic in Fig. 3.

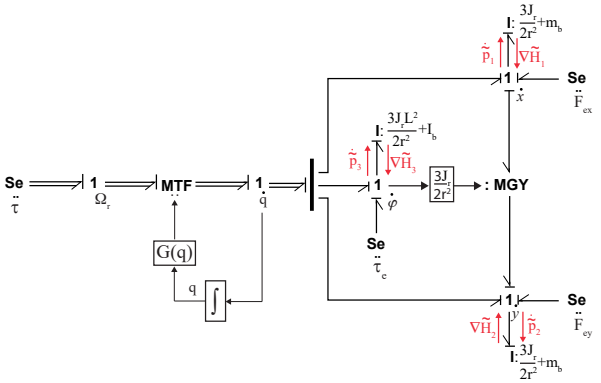

Fig. 3: Mobile base BG scheme with inertia regrouping.

The correspondence of this BG with the results of force-balance and EL modeling is clearly suggested considering equation (7) and comparing its main components given in (8), the inertia matrix M with the parameters of the I-elements of the BG, and the entries of the matrix $C(q,\dot{q})$ with the coefficient modulating the gyrator MGY.

The BG-EL equivalence can be more formally established deriving the EL equations from the BG of Fig. 2 following the procedure given in [12]. This is not presented here due to lack of space.

B. Residual Sinks and Lagrange multipliers

Another way to avoid DC is to enforce IC in all energy storage elements by using *residual sinks*. Starting from the BG in Fig. 2, the procedure consists on incorporating effort sources through **0**-junctions into the storage elements in DC, as observed in Fig. 4.

The *residual sinks* inject the necessary effort into the **0**-junctions to ensure that the net flow through them is zero. Thus, defining $f_{\text{vir}} := [f_{\text{vir1}},\ f_{\text{vir2}},\ f_{\text{vir3}}]^T$, the flow balance equations in the **0**-junctions are

$$\begin{aligned}\mathbf{0}_{3\times 1} &= f_{vir}\\ &= G(q)^T\dot{q} - \Omega_r\\ &= A(\psi)^T\dot{\psi}\end{aligned}$$

Thus, we can see that the constraint matrix $A(\psi)$, of equation (12), can be obtained by enforcing IC for all energy storage elements in DC through the incorporation of *residual sinks*.

Remark 4. The efforts introduced by the *residual sinks* are equivalent to the Lagrange multipliers vector λ defined in (10), so they can be interpreted physically as the force that the ground must exert to fulfill the perfect rolling condition defined in (2). This force is hidden in the final model obtained through the BG modeling and both, the EL and pHS modeling.

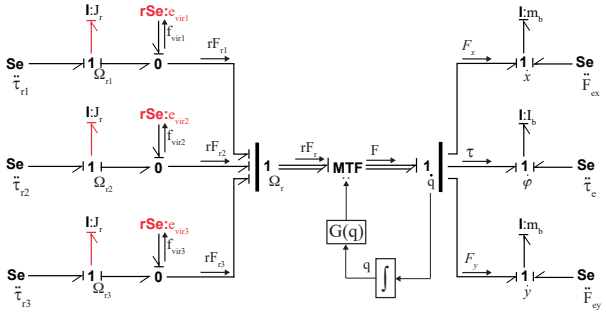

Fig. 4: Mobile base BG scheme with *residual sinks*.

C. Bond Graph - Hamiltonian System

The pHS model can be obtained through the manipulation of the BG using the method developed in [13]. Alternatively, in this simple case, the pHS is obtained applying the state-equations derivation procedure writing the derivatives of the state variables, i.e. the inputs of the storage elements, as functions of their outputs, as these are the components of the gradient of the stored energy (please refer to the red signals marked in Fig. 3).

D. Passivity

The power delivered to the system (21) is

$$\begin{aligned}u^T y &= u^T g(\boldsymbol{x})^T \nabla\tilde{H}(\boldsymbol{x})\\ &= \left(\dot{\boldsymbol{x}} - J(\boldsymbol{x})\nabla\tilde{H}(\boldsymbol{x})\right)^T \nabla\tilde{H}(\boldsymbol{x})\\ &= \dot{\boldsymbol{x}}^T\nabla\tilde{H}(\boldsymbol{x})\\ &= \dot{\tilde{H}}(\boldsymbol{x})\end{aligned}$$

where it was taken into account that

$$\frac{\partial\tilde{H}}{\partial\tilde{p}}^T C(q,\dot{q})\frac{\partial\tilde{H}}{\partial\tilde{p}} = 0$$

Since the following inequality is satisfied

$$\underbrace{\tilde{H}(\boldsymbol{x}(t)) - \tilde{H}(\boldsymbol{x}(0))}_{\text{stored energy}} \leq \underbrace{\int_0^t u(s)^T y(s)ds}_{\text{delivered energy}}$$

the system is cyclo-passive [4]. Moreover, since $\tilde{H}(\boldsymbol{x}) \geq 0$, the system is also passive.

Remark 5. In both the EL and pHS modeling, we started with the generalized configuration coordinates ψ of dimension 6, and after some algebraic work, the model ended up being expressed in terms of the posture coordinates vector q of dimension 3. This conclusion can be quickly reached by analyzing the causalized BG model in Fig. 2. Even if all the configurations coordinates ψ appear in the model, the number of energy storage elements in IC is 3.

IV. Controller Design

Elaborating on the compact version of the BG scheme shown in Fig. 3 in this section we propose a PID-velocity

control scheme that can be an objetive per-se or an inner-loop of a position controller. The PID can be represented in the energy domain as a combination of dissipative and (kinetic and potential) storage elements, as shown in Fig. 5. The external passivity between its input (the velocity error) and its output (the torque vector commanding the wheels) can be easily verified. The velocity input references Ω_r^* can be expressed as function of the desired mobile base velocities $\dot{q}^*$ using the relation of equation (3), i.e., $\Omega_r^* = G(q)^T \dot{q}^*$. Then, the resulting control law is

$$\tau = -K_P \tilde{\Omega}_r - K_I \tilde{\theta}_r - K_D \dot{\tilde{\Omega}}_r$$

where $\tilde{\Omega}_r = \Omega_r - \Omega_r^*$ is the velocity error, $\tilde{\theta}_r = \int \tilde{\Omega}_r$ and K_P, K_I and K_D are positive definite diagonal matrices, each (3×3) dimensional.

Exploiting the BG-pHS correspondence, we study the stability of the closed-loop equilibrium point $(\tilde{\theta}_{r*} = 0, \tilde{\Omega}_{r*} = 0, \tilde{p}_* = 0)$ proposing the sum of the PID-associated energy function and the Hamiltonian (19) as the candidate Lyapunov function

$$V(\tilde{\theta}_r, \tilde{\Omega}_r, \tilde{p}) = \frac{1}{2}\tilde{\theta}_r^T K_I \, \tilde{\theta}_r + \frac{1}{2}\tilde{\Omega}_r^T K_D \, \tilde{\Omega}_r + \frac{1}{2}\tilde{p}^T M^{-1} \tilde{p}$$

From (20), considering that $\tilde{p} = M\dot{q}$ and considering $h_e = \mathbf{0}_{3\times 1}$, the time derivative of V is

$$\begin{aligned}\dot{V} &= \tilde{\theta}_r^T K_I \, \dot{\tilde{\theta}}_r + \tilde{\Omega}_r^T K_D \, \dot{\tilde{\Omega}}_r + \tilde{p}^T M^{-1} \dot{\tilde{p}} \\ &= -\tilde{\Omega}_r^T \tau - \tilde{\Omega}_r^T K_P \tilde{\Omega}_r + \tilde{p}^T M^{-1} \left(G(q)\tau - C(q,\dot{q}) \frac{\partial \tilde{H}}{\partial \tilde{p}} \right) \\ &= -\tilde{\Omega}_r^T K_P \tilde{\Omega}_r\end{aligned}$$

As $\dot{V}$ is negative semi-definite, it cannot be guaranteed that the equilibrium point is asymptotically stable.

The latter can be easily proved invoking La Salle's invariance principle and analyzing the closed-loop dynamics when the input $\Omega_r^* = 0$. As the system continues evolving, the equilibrium point is asymptotically stable.

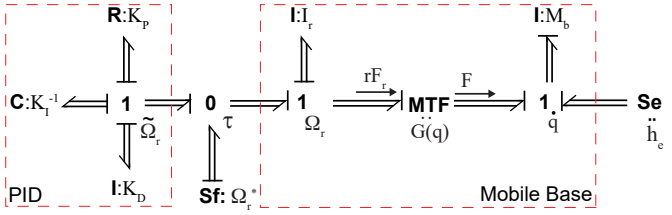

Fig. 5: PID controller BG scheme.

V. Conclusions

In this work, the kinematic and dynamic models of an omnidirectional base with three omni wheels were presented. The dynamic model was developed using four different techniques: BG, Force Balance, EL, and pHS. The first one was used as a *lingua franca* for the generalization of results. The manipulation of the BG model to avoid derivative causalities and its linking with the EL model allowed to explicitly express and give a mathematical meaning to the Lagrange multipliers, demonstrating that these were equivalent to the forces introduced by the *residual sinks*. With both methodologies, these forces disappeared in the final model. At the same time, it was demonstrated that both can be interpreted physically as the force that the ground must exert to fulfill the perfect rolling condition. Finally, a PID-velocity control design was presented.

Acknowledgment

The authors wish to thank the National University of Rosario for funding this work through the projects PPCT-80020220600083UR and PID-80020190300098UR.

References

[1] T. INCOSE, "Systems engineering vision 2020," *INCOSE, San Diego, CA, accessed Jan*, vol. 26, no. 2019, p. 2, 2007.

[2] G. Barbieri, K. Kernschmidt, C. Fantuzzi, and B. Vogel-Heuser, "A sysml based design pattern for the high-level development of mechatronic systems to enhance re-usability," *IFAC Proceedings Volumes*, vol. 47, no. 3, pp. 3431–3437, 2014.

[3] R. Ortega, J. A. L. Perez, P. J. Nicklasson, and H. J. Sira-Ramirez, "Introduction," in *Passivity-based control of Euler-Lagrange systems: mechanical, electrical and electromechanical applications*. Springer Science & Business Media, 2013, ch. 1, pp. 1–15.

[4] A. Van der Schaft, *L2-gain and passivity techniques in nonlinear control*. Springer, 2000, vol. 2.

[5] D. C. Karnopp, D. L. Margolis, and R. C. Rosenberg, *System dynamics: modeling, simulation, and control of mechatronic systems*. John Wiley & Sons, 2012.

[6] A. Donaire and S. Junco, "Energy shaping, interconnection and damping assignment, and integral control in the bond graph domain," *Simulation Modelling Practice and Theory*, vol. 17, no. 1, pp. 152–174, 2009.

[7] A. Achir, S. Junco, A. Donaire, and C. Sueur, "A bond-graph method for flatness-based dynamic feedback linearization controller synthesis: Application to a current-fed induction motor," in *ECMS '06*, 2006.

[8] C. C. de Wit, B. Siciliano, and G. Bastin, *Theory of robot control*. Springer Science & Business Media, 2012.

[9] R. Ram, P. Pathak, and S. Junco, "Trajectory control of a mobile manipulator in the presence of base disturbance," *SIMULATION*, vol. 95, no. 6, pp. 529–543, 2019.

[10] M. M. Gor, P. M. Pathak, A. K. Samantaray, J. M. Yang, and S. W. Kwak, *Bond graph Modeling and Control of Compliant Legged Quadruped Robot*. Cham: Springer International Publishing, 2017, pp. 497–546.

[11] M. Nacusse, M. Crespo, S. Junco, V. Rayankula, and P. M. Pathak, "Bond graph model conditioning for analysis, simulation and control system design: Application to a planar mobile robotic manipulator," in *IMAACA*, 2017.

[12] D. Karnopp, "Lagrange's Equations for Complex Bond Graph Systems," *Journal of Dynamic Systems, Measurement, and Control*, vol. 99, no. 4, pp. 300–306, 12 1977.

[13] A. Donaire and S. Junco, "Derivation of input-state-output port-hamiltonian systems from bond graphs," *Simulation Modelling Practice and Theory*, vol. 17, no. 1, pp. 137–151, 2009.

[14] V. Duindam, A. Macchelli, S. Stramigioli, and H. Bruyninckx, *Modeling and Control of Complex Physical Systems: The Port-Hamiltonian Approach*. Springer Berlin Heidelberg, 2009.

[15] B. Siciliano, L. Sciavicco, L. Villani, and G. Oriolo, "Motion control," in *Robotics: modelling, planning and control*. Springer Science & Business Media, 2009, ch. 11, pp. 369–521.

[16] R. Fierro and F. L. Lewis, "Control of a nonholomic mobile robot: Backstepping kinematics into dynamics," *Journal of robotic systems*, vol. 14, no. 3, pp. 149–163, 1997.

[17] G. Wanner and E. Hairer, *Solving ordinary differential equations II*. Springer Berlin Heidelberg New York, 1996, vol. 375.

[18] W. Borutzky and F. E. Cellier, "Tearing algebraic loops in bond graphs," *Transactions of the Society for Computer Simulation International*, vol. 13, no. 2, p. 102–115, Dec 1996.